Empirical comparison between effective medium theory models for the dielectric response of biological tissue at terahertz frequencies

GORETTI G. HERNANDEZ-CARDOSO[1], ABHISHEK K. SINGH[1], AND ENRIQUE CASTRO-CAMUS[1,*]

[1] Centro de Investigaciones en Optica A.C., Loma del Bosque 115, Lomas del Campestre, Leon, Guanajuato 37150, Mexico
[*] Corresponding author: enrique@cio.mx

Compiled December 11, 2019

We study the use of three effective medium theory models, namely, Maxwell-Garnett, Bruggeman and Landau-Lifshitz-Looyenga, for the dielectric response of biological tissue in the terahertz band of the electromagnetic spectrum. In order to accomplish our objectives, we performed measurements on water-dehydrated basil binary mixtures encompassing the entire concentration range and we further analyze the dielectric function with the models. Our results indicate that the Landau-Lifshitz-Looyenga and Bruggeman models provide marginally better fit to the experimentally measured dielectric function in the terahertz band. We further discuss the biological relevance of the models in the context of our experimental data based on their fundamental assumptions.

This is a pre-print, the final version can be found in https://doi.org/10.1364/AO.382383

1. INTRODUCTION

In recent years, the number of applications of terahertz radiation has increased, ranging from industry [1] to biology [2–6] and medicine [7–10]. Given the fact that the timescales of water collective dynamics fall exactly in the terahertz (THz) band, this type of radiation is very sensitive to the hydration changes in materials.

Effective medium theory (EMT) models provide an analytical approach to calculate the macroscopic complex dielectric properties of materials by employing the dielectric properties of their constituents and their volume fractions [11]. The models based on the effective medium theory provide analytical expressions for the optical properties of the complex systems making some assumptions. Since, there are a range of effective medium models that, in general differ, a particular one has to be chosen in order to analyze a given system. The frequently used models based on the effective medium theory in order to analyze a biological system at terahertz frequencies are Maxwell-Garnett, Bruggeman, and Landau-Lifshitz-Looyenga [12, 13].

A. Maxwell-Garnett

The Maxwell-Garnett (MG) is a traditional model based on EMT that estimates the aggregate dielectric function of the complex system as

$$\varepsilon_{\text{eff}} = \varepsilon_h \frac{2X_p\left(\varepsilon_p - \varepsilon_h\right) + \left(\varepsilon_p + 2\varepsilon_h\right)}{\left(2\varepsilon_h + \varepsilon_p\right) + X_p\left(\varepsilon_h - \varepsilon_p\right)}, \tag{1}$$

where ε_h is the dielectric function of the host material, ε_p is that of the guest material, and X_p is the guest's volume fraction.[14] It is to be noted that this formulation is asymmetric in such a way that if the host and guest materials are exchanged the effective dielectric function ε_{eff} would be different. The asymmetry enhances when difference in the dielectric functions of the constituents is large [14]. In addition, as the volumetric fraction of the inclusions increases, the assumptions are violated as the effective dielectric function changes. Therefore, this model is valid for low solute concentrations [15].

B. Bruggeman

The Bruggeman (BM) model is an improved version of MG model, and consists of a two-component homogeneous system for the effective dielectric function ε_{eff} given by [14]

$$\varepsilon_{\text{eff}} = \frac{1}{4}\left(\beta + \sqrt{\beta^2 + 8\varepsilon_h\varepsilon_p}\right), \tag{2}$$

where

$$\beta = \left(3X_h - 1\right)\varepsilon_h + \left(3X_p - 1\right)\varepsilon_p,$$

with X_h, ε_h and X_p, ε_p are volumetric fractions and dielectric functions of the individual components, and $X_h + X_p = 1$. The BM theory is also based on spherical approximation for the guest (solute) but, in contrast to MG model, it is symmetric [14] and allows a large contrast of the components dielectric function for the complex system [15].

C. Landau-Lifshitz-Looyenga

The Landau-Lifshitz-Looyenga (LLL) model assumes a medium composed by a host and a guest. The LLL equation is given by [16]

$$\sqrt[3]{\varepsilon_{\text{eff}}} = X_h \sqrt[3]{\varepsilon_h} + X_p \sqrt[3]{\varepsilon_p} \quad (3)$$

where $X_{h(p)}$ and $\varepsilon_{h(p)}$ denote the volumetric fraction and the complex dielectric function of the host and guest, respectively, and $X_h + X_p = 1$.

Unlike the models described above, this theory allows arbitrarily shaped particles [17] but, it is, in principle, inappropriate to describe the optical properties of a system in which its components have large dielectric contrast [15]. It is worth mentioning that for biological tissue it is hard to define the size or shape of an inclusion, since biological tissue presents mesoscopic (pores, vasculature, etc.) and microscopic (cells, membranes, proteins, etc.) structure and water is distributed in between this plethora of structural features.

We provide a comparative analysis of the aforementioned models for the determination of water content in biological tissues from terahertz spectroscopic measurements. In order to accomplish this, we prepared binary mixtures of dehydrated and ground *Ocimum basilicum* (basil) tissue and water, which we consider a model system with terahertz dielectric properties similar to a range of soft biological tissues. The measurements were performed throughout the host/guest volumetric fraction range (0.0 - 1.0) employing terahertz time-domain spectroscopy within the frequency range of 0.3 THz to 0.4 THz. A quantitative analysis is provided by calculating the error between experimental and theoretical data, as well as by using least squares adjustments of the experimental data by the three models.

2. METHODS

In the attempt to model biological tissue, nine mixtures of pure water and dry basil powder with different water volumetric concentrations (0.1 - 0.9) were prepared. Besides, a sample of pure water and one of dehydrated basil were considered. Terahertz measurements were made with a Picometrix spectrometer in reflection geometry. The mixtures were placed onto a polyethylene window in a kinematic optical mount, making sure to avoid air bubbles that could influence the optical properties of the sample. Reference and sample waveforms were recorded for each mixture. Ten thousand waveforms were averaged for each measurement.

A. Determination of the dielectric function of dehydrated basil

Basil leaves were dehydrated and grounded to powder. The basil powder was used to form five pellets under a pressure of 4 MPa resulting in thicknesses between 1.04 mm and 1.79 mm. With terahertz time-domain spectroscopy, the transmittance of the basil pellet was measured in a nitrogen environment, in order to avoid the water vapor contribution. The data were processed in order to obtain the dielectric function as described in Ref. [18]. The real and imaginary parts of the complex dielectric function are shown in Fig. 1. Second order polynomials were fitted to both parts of the complex dielectric function. The dielectric function of the dehydrated basil can then be approximated by

$$\varepsilon_R = -0.15\,\text{THz}^{-2} f^2 + 0.16\,\text{THz}^{-1} f + 3.16 \quad (4)$$

and

$$\varepsilon_I = -0.01\,\text{THz}^{-2} f^2 + 0.17\,\text{THz}^{-1} f + 0.03 \quad (5)$$

where f is the frequency in THz.

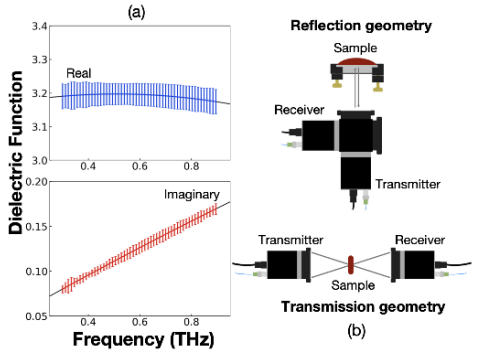

Fig. 1. (a) Complex dielectric function of dehydrated basil. Dehydrated basil pellets were measured in a nitrogen environment. Second order polynomials were fitted to the data obtained from five different pellets. The error bars represent the standard deviation of the five measurements. (b) Scheme of the THz measurements. Reflection geometry was employed to measure the water–basil mixtures. The dry basil pellets measurements were recorded in transmission geometry.

In order to theoretically compare the EMT models, the calculated basil dielectric function, Eq. 4 and Eq. 5, and the water dielectric function given by the double Debye model in [19] were used to determine the dielectric function of the water-basil medium for different hydration degrees (Figure 2).

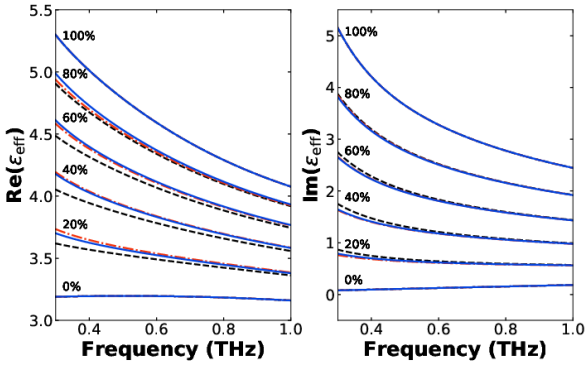

Fig. 2. Complex dielectric function of water-basil mixture for various hydration degrees given by MG (black dashed lines), BM (red dash-dotted lines) and LLL (blue solid lines) models in the frequency range from 0.3 THz to 1.0 THz.

B. Water-basil mixture preparation

In order to compare the EMT models with experimental data, binary mixtures of water and dehydrated basil powder were prepared by encompassing the entire concentration range. A basil powder was prepared by dehydrating leaves collected from living plants, and grinding them with a mortar and pestle into a fine powder. The hydrated samples were prepared by mixing a known weight of powder with a known volume of water taking into consideration the respective densities as described in the

following paragraph. The mass fractions were calculated from volumetric fraction of water by [4]

$$W_w = \frac{X_w \rho_w}{X_w \rho_w + X_s \rho_s}, \quad (6)$$

where

$$M_w = W_w M_t \quad (7)$$

and

$$M_s = (1 - W_w) M_t, \quad (8)$$

where $\rho_w = 997\,\mathrm{kg/m^3}$ is the density of water and $\rho_s = 1099.89\,\mathrm{kg/m^3}$ is the density of the dehydrated basil, W_i denotes the mass fraction, X_i the volumetric fraction, ρ_i the density, M_i the mass of the component and M_t the total mass of the mixture. The suffixes w and s correspond to water and solid/dry tissue, respectively.

C. Determination of complex dielectric function

The comparison among the EMT models and the experimental data was performed by determining the error in the dielectric function.

Measurements were made with THz-TDS in order to obtain the mixtures complex dielectric function. A picometrix teragauge system was used in reflection geometry. The mixtures were placed onto a high density polyethilene (HDPE) window in a kinematic optical mount. A reference electric field $E_{ref}(t)$ was recorded in the absence of sample. Subsequently the sample was placed and the reflected electric field $E_{sam}(t)$ was recorded again. In reflection geometry, the recorded signals are composed of two pulses, the first E_1 comes from the reflection in the air-window interface, while the second E_2 corresponds to the reflection from window-sample interface. Then, the complex refractive index was obtained as described in Ref. [20]. For normal incidence, the expressions to determine the complex refractive index are reduced to

$$\tilde{n}_{sam} = \frac{n_{win}(1 - r_{sam})}{1 + r_{sam}}, \quad (9)$$

where

$$r_{sam} = \frac{H_{sam}}{H_{ref}} r_{air}. \quad (10)$$

n_{win} is the refractive index of the HDPE window, $r_{air} = (n_{win} - 1)/(n_{win} + 1)$ and $H_{sam(ref)}$ is given by the ratio of $\tilde{E}_{2,sam(ref)}(\omega)$ and $\tilde{E}_{1,sam(ref)}(\omega)$ which are the Fourier transforms of the electric pulses obtained from the sample and reference as explained above. Theoretically, the dielectric function corresponding to each sample concentration was determined by the MG, BM and LLL models.

D. Transfer function for reflection measurements and fitting of theoretical models

The quantification of water in the water-basil mixtures was performed via curve fitting to the transfer function. From the samples' measurements, the experimental transfer function H_{exp} can be obtained as

$$H_{exp} = \left| \frac{\tilde{E}_{2,sam}}{\tilde{E}_{1,sam}} \right|. \quad (11)$$

The corresponding theoretical transfer function can be calculated as

$$H_{theo} = \frac{r_{mix}}{r_{air}} |H_{air}|, \quad (12)$$

where r_{air} is defined in the previous section, H_{air} is calculated using Eq. 11 in the absence of sample [21], and r_{mix} is the refraction coefficient from the sample given by

$$r_{mix} = \frac{n_{win} - \sqrt{\varepsilon_{mix}(X_w)}}{n_{win} + \sqrt{\varepsilon_{mix}(X_w)}}. \quad (13)$$

ε_{mix} is calculated for each of the EMT models for the volumetric fraction X_w that water occupies in the mixture. Least square method was used to fit H_{theo} to data H_{exp} in order to obtain the optimal value for X_w. In recent years the subtle deviations of the dielectric function of aqueous solutions of biomolecules from the predicted EMT at different concentrations has shown the sensitivity of terahertz spectroscopy to the presence of a third component in the mixture, namely bound water,[22] yet, the difference in the dielectric properties of bulk water and bound water is only of the order of 2 % and is dependent on the solute, which means that making a distinction between these two components in a tissue mixture is unnecessary for the purposes of water content determination.

3. RESULTS

A. Complex dielectric function *vs.* water volumetric fraction

The theoretical dielectric function was obtained as a function of the water volumetric fraction for each of the EMT models under consideration. In the Figure 3 these curves are shown as solid black, red and blue lines corresponding to MG, BM and LLL theories, respectively. The grey dots represent the experimental dielectric functions of the mixtures. From the figure, we can observe that, although the experimental dielectric function coincides reasonably well with the theoretical curves, they overlap each other, making it difficult to define which of the models fits better the experimental data.

In order to quantitatively evaluate the three EMT models, the deviation between the experimental and theoretical dielectric function at 0.4 THz was obtained. The real and imaginary dielectric function values are summarized in Tables 1 and 2, respectively.

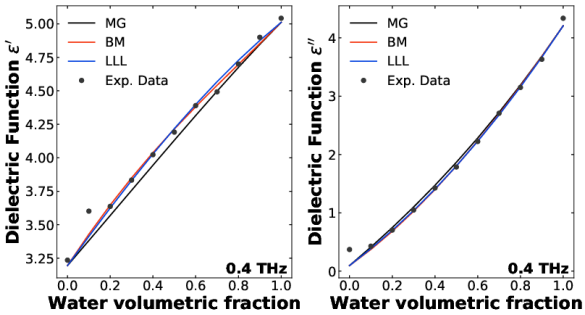

Fig. 3. Real and imaginary part of the dielectric function of water-basil mixture as a function of the water volumetric fraction at 0.4 THz. The solid lines in black, red and blue show the mixture's theoretical dielectric function given by the MG, BM and LLL models, respectively. The grey dots represent the experimental data.

B. Transfer function

The transfer function, which describes the response of the sample to the terahertz signal, was determined theoretically and

X_w	Exp.	MG	Δ	BM	Δ	LLL	Δ
0.0	3.24	3.20	0.04	3.20	0.04	3.20	0.04
0.1	3.60	3.38	0.22	3.43	0.17	3.41	0.19
0.2	3.64	3.57	0.07	3.65	0.01	3.62	0.02
0.3	3.83	3.76	0.07	3.85	0.02	3.83	0.00
0.4	4.02	3.94	0.08	4.04	0.02	4.03	0.01
0.5	4.19	4.13	0.06	4.21	0.02	4.22	0.03
0.6	4.39	4.32	0.07	4.38	0.01	4.40	0.01
0.7	4.49	4.50	0.01	4.54	0.05	4.57	0.08
0.8	4.70	4.67	0.03	4.70	0.00	4.73	0.03
0.9	4.90	4.85	0.05	4.85	0.05	4.88	0.02
1.0	5.04	5.01	0.03	5.01	0.03	5.01	0.03
Average			0.07		0.04		0.04

Table 1. Real part of the water-basil complex dielectric function resulting from the experimental measurements and the EMT models at 0.4 THz. The corresponding deviations are shown for the mixtures, as well as the average per model.

X_w	Exp.	MG	Δ	BM	Δ	LLL	Δ
0.0	0.37	0.10	0.27	0.10	0.28	0.10	0.28
0.1	0.43	0.41	0.02	0.37	0.06	0.38	0.04
0.2	0.70	0.75	0.05	0.68	0.02	0.70	0.01
0.3	1.05	1.10	0.05	1.03	0.02	1.04	0.01
0.4	1.43	1.47	0.04	1.40	0.03	1.41	0.02
0.5	1.79	1.87	0.08	1.80	0.02	1.80	0.02
0.6	2.22	2.28	0.06	2.23	0.01	2.23	0.00
0.7	2.71	2.73	0.02	2.69	0.02	2.68	0.03
0.8	3.15	3.19	0.04	3.17	0.02	3.16	0.01
0.9	3.63	3.69	0.06	3.68	0.05	3.67	0.04
1.0	4.34	4.21	0.13	4.21	0.13	4.21	0.13
Average			0.08		0.06		0.05

Table 2. Imaginary part of the water-basil complex dielectric function resulting from the experimental measurements and the EMT models at 0.4 THz. The corresponding deviations are shown for the mixtures, as well as the average per model.

experimentally. The same experimental data shown previously were processed slightly differently from the dielectric function, as described in the methods section. In the previous procedure, theoretical curves of the transfer function for each EMT model were obtained, as well as the experimental transfer function for all the measured mixtures. In Figure 4 we can appreciate the experimental data as grey points and the theoretical curves as solid black, red and blue lines for the MG, BM and LLL models, respectively. The data is presented only on the 300 GHz to 400 GHz band since this is the part of the spectrum in which our TDS system has the best signal to noise performance.

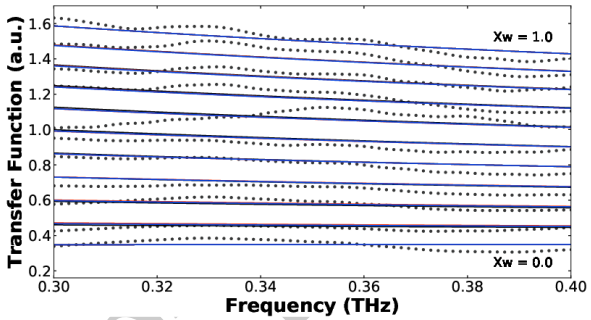

Fig. 4. Experimental (grey dots) and theoretical (solid lines) transfer function of mixtures.

C. Quantification of water in biological tissue: the inverse problem

In order to obtain the hydration degree of a biological medium from the THz measurements, a relationship between the hydration level of tissue and its terahertz optical properties is built and it is shown in Figure 2. Since the biological tissue is considered as the combination of dehyrated tissue and water and given that the complex dielectric properties of both components are known, the water content in a sample is found by fitting a theoretical function dependent on X_w to the experimental data.

In this study, with the purpose to fully evaluate the three EMT models, a least squares fit algorithm was used to measure the water content in the prepared mixtures. The theoretical transfer function, given by Eq. 12, was fitted to its corresponding experimental transfer function. The optimal value for X_w such that H_{theo} fits H_{exp} best determines the hydration degree in the sample. The values predicted by MG, BM and LLL models in all the mixtures are shown in Table 3.

4. DISCUSSION

As seen in Fig. 2, there are differences in the dielectric functions resulting from the three different models being BM and LLL closer to each other than MG. This is consistent with the single-frequency comparison, at 400 GHz, shown in Fig. 3, where experimental data from our mixtures is also presented. In the plot it is possible to see that BM and LLL approximates the experimental data marginally better for most concentrations, those results are summarized quantitatively in tables 1 and 2. The comparison of the three models and the experimental data across the spectral band from 300 GHz to 400 GHz presented in Fig. 4 that the differences among the three models and, also, the experimental data are small. The measured transfer function shows some oscillations around the theoretical curves, most

Mixture	MG	Δ	BM	Δ	LLL	Δ
1.0	1.01	0.01	1.01	0.01	1.01	0.01
0.9	0.92	0.02	0.92	0.02	0.92	0.02
0.8	0.81	0.01	0.81	0.01	0.81	0.01
0.7	0.71	0.01	0.71	0.01	0.71	0.01
0.6	0.60	0.00	0.60	0.00	0.60	0.00
0.5	0.47	0.03	0.47	0.03	0.47	0.03
0.4	0.38	0.02	0.38	0.02	0.38	0.02
0.3	0.27	0.03	0.27	0.03	0.27	0.03
0.2	0.21	0.01	0.20	0.00	0.20	0.00
0.1	0.09	0.01	0.08	0.02	0.08	0.02
0.0	0.00	0.00	0.00	0.00	0.00	0.00
Average		0.01		0.01		0.01

Table 3. Water volumetric fractions resulting from the least squares fitting of the MG, BM and LLL theoretical curves to the experimental data. The corresponding deltas are shown for the mixtures.

likely caused by spurious reflections in the spectroscopy setup that introduce Fabry-Perot spectral oscillations. In Table 3, the results from fitting the experimental spectra with the three models are shown, demonstrating that the outcome of all three models for the inverse problem are comparably good and acceptable with an average deviation of about 1%.

A characteristic of biological tissue in the terahertz regime is the high contrast between the dielectric functions of water and the rest of the tissue, besides the variability in shape of the particles considered as background tissue. These factors together complicate the decision to select one model over another, for the analysis of the optical properties for biological tissues. For instance, the Maxwell-Garnett theory restricts the particles to be spherical in shape, in addition it is asymmetric, particularly when there is a large difference in the dielectric constants of the compounds. Bruggeman model allows higher contrasts between dielectric functions of the components but is also restricts the particles to be spherical in shape. Landau-Lifshitz-Looyenga model is a good choice if the mixture consists of irregularly shaped components, however, it is only, in principle, applicable if contrast in dielectric function of the components is limited, therefore biological tissue does not fully comply with the construction assumptions of any of them.

The high contrast in the dielectric functions contradicts the hypothesis of the MG and LLL models, unlike the BM model that allows great differences in the permittivity. However, the shape of the dry tissue particles is irregular, this contradicts the hypotheses of the MG and BM models that are restricted to spherical particles, being the LLL model the only one among the considered models that allows arbitrarily shaped particles.

From the results shown, in spite of not fulfilling the construction hypothesis of the models, the three of them behave empirically well, fitting adequately the experimental data. Based on the fitting to the transfer function, all the three models are appropiate for the hydration quantification. From the calculation of the dielectric function error, we found that the LLL and BM models are more suitable for modeling biological tissue in the terahertz range.

5. CONCLUSIONS

In this work we study the applicability of models based on the effective medium theory to biological tissues in the terahertz band. We choose water-basil mixture as a model controllable samples of biological tissues. Three models, namely, Maxwell-Garnett, Bruggeman, and Landau-Lifshitz-Looyenga based on the effective medium theory were compared. Water-basil mixtures were prepared by varying the volume fraction of the components. Both the complex dielectric function and the transfer function of the mixtures were obtained using the THz-TDS technique. The experimental data were compared with the corresponding theoretical curves determined by the effective medium theory models. The results obtained indicate that all three models qualitatively fit the experimental data. However, the LLL and BM theories are quantitatively the more suitable for modeling biological tissues in the terahertz regime.

Funding Information. Consejo Nacional de Ciencia y Tecnologia (CONACYT) (294440)

Author Contributions. The study was conceived an supervised by ECC. GGHC performed the experiments, data analysis with support of AKS and ECC. GGHC and AKS wrote the manuscript jointly. All authors reviewed the manuscript.

Disclosures. The authors declare no conflicts of interest.

REFERENCES

1. A. I. Hernandez-Serrano, S. C. Corzo-Garcia, E. Garcia-Sanchez, M. Alfaro, and E. Castro-Camus, "Quality control of leather by terahertz time-domain spectroscopy," Appl. Opt. **53**, 7872–7876 (2014).
2. S. W. Smye, J. M. Chamberlain, A. J. Fitzgerald, and E. Berry, "The interaction between terahertz radiation and biological tissue," Phys. Medicine Biol. **46**, R101–R112 (2001).
3. P. H. Siegel, "Terahertz technology in biology and medicine," IEEE Transactions on Microw. Theory Tech. **52**, 2438–2447 (2004).
4. R. Gente, N. Born, N. Voß, W. Sannemann, J. Léon, M. Koch, and E. Castro-Camus, "Determination of leaf water content from terahertz time-domain spectroscopic data," J. Infrared, Millimeter, Terahertz Waves **34**, 316–323 (2013).
5. E. Castro-Camus, M. Palomar, and A. A. Covarrubias, "Leaf water dynamics of arabidopsis thaliana monitored in-vivo using terahertz time-domain spectroscopy," Sci. Reports **3**, 2910 EP – (2013).
6. L. Guo, X. Wang, P. Han, W. Sun, S. Feng, J. Ye, and Y. Zhang, "Observation of dehydration dynamics in biological tissues with terahertz digital holography," Appl. optics **56**, F173–F178 (2017).
7. E. Pickwell and V. P. Wallace, "Biomedical applications of terahertz technology," J. Phys. D: Appl. Phys. **39**, R301–R310 (2006).
8. G. G. Hernandez-Cardoso, S. C. Rojas-Landeros, M. Alfaro-Gomez, A. I. Hernandez-Serrano, I. Salas-Gutierrez, E. Lemus-Bedolla, A. R. Castillo-Guzman, H. L. Lopez-Lemus, and E. Castro-Camus, "Terahertz imaging for early screening of diabetic foot syndrome: A proof of concept," Sci. Reports **7**, 42124 EP – (2017).
9. M. Borovkova, M. Khodzitsky, P. Demchenko, O. Cherkasova, A. Popov, and I. Meglinski, "Terahertz time-domain spectroscopy for non-invasive assessment of water content in biological samples," Biomed. Opt. Express **9**, 2266–2276 (2018).
10. B. C. Truong, A. J. Fitzgerald, S. Fan, and V. P. Wallace, "Concentration analysis of breast tissue phantoms with terahertz spectroscopy," Biomed. optics express **9**, 1334–1349 (2018).
11. X. C. Zeng, D. J. Bergman, P. M. Hui, and D. Stroud, "Effective-medium theory for weakly nonlinear composites," Phys. Rev. B **38**, 10970–10973 (1988).

12. J. F. Federici, "Review of moisture and liquid detection and mapping using terahertz imaging," J. Infrared, Millimeter, Terahertz Waves **33**, 97–126 (2012).
13. M. Scheller, S. Wietzke, C. Jansen, and M. Koch, "Modelling heterogeneous dielectric mixtures in the terahertz regime: a quasi-static effective medium theory," J. Phys. D: Appl. Phys. **42**, 065415 (2009).
14. T. C. Choy, *Effective Medium Theory Principles and Applications* (Oxford Science Publications, 1999).
15. M. Scheller, C. Jansen, , and M. Koch, "Applications of effective medium theories in the terahertz regime," in *Recent Optical and Photonic Technologies,* K. Y. Kim, ed. (IntechOpen, Rijeka, 2010), chap. 12.
16. H. Looyenga, "Dielectric constants of heterogeneous mixtures," Physica. **31**, 401 – 406 (1965).
17. S. O. Nelson, "Density-permittivity relationships for powdered and granular materials," IEEE Transactions on Instrumentation Meas. **54**, 2033–2040 (2005).
18. E. Castro-Camus and M. B. Johnston, "Extraction of the anisotropic dielectric properties of materials from polarization-resolved terahertz time-domain spectra," J. Opt. A: Pure Appl. Opt. **11**, 105206 (2009).
19. H. J. Liebe, G. A. Hufford, and T. Manabe, "A model for the complex permittivity of water at frequencies below 1 thz," Int. J. Infrared Millim. Waves **12**, 659–675 (1991).
20. P. U. Jepsen, "Determining parameters of the dielectric function of a substance in aqueous solution by self-referenced reflection thz spectroscopy," US Pat. 8374800 (2013).
21. P. U. Jepsen, U. Møller, and H. Merbold, "Investigation of aqueous alcohol and sugar solutions with reflection terahertz time-domain spectroscopy," Opt. Express **15**, 14717–14737 (2007).
22. M. Heyden, E. Bründermann, U. Heugen, G. Niehues, D. Leitner, and M. Havenith, "Long-range influence of carbohydrates on the solvation dynamics of water-answers from terahertz absorption measurements and molecular modeling simulations," J. Am. Chem. Soc. **130**, 5773–5779 (2008).